LETTER

Solitary waves and localized nonlinear excitations in the strongly nonlinear β-Fermi-Pasta-Ulam-Tsingou chain

To cite this article: Alexandra Westley and Surajit Sen 2018 *EPL* **123** 30005

A Letters Journal Exploring the Frontiers of Physics

August 2018

EPL, **123** (2018) 30005 www.epljournal.org
doi: 10.1209/0295-5075/123/30005

Solitary waves and localized nonlinear excitations in the strongly nonlinear β-Fermi-Pasta-Ulam-Tsingou chain

Alexandra Westley and Surajit Sen

Physics Department, State University of New York at Buffalo - Buffalo, NY 14260-1500, USA

received 17 January 2018; accepted in final form 7 August 2018
published online 4 September 2018

PACS 05.90.+m – Other topics in statistical physics, thermodynamics, and nonlinear dynamical systems
PACS 05.45.-a – Nonlinear dynamics and chaos
PACS 05.70.Ln – Nonequilibrium and irreversible thermodynamics

Abstract – We develop new analytic descriptions for solitary waves (SWs) and SW-like objects in the non-integrable and strongly nonlinear β-Fermi-Pasta-Ulam-Tsingou (β-FPUT) system for various strengths of the harmonic term in the potential. We then show that that the collision of identical solitary waves in the decorated β-FPUT chain can lead to the formation of one or more long-lived localized nonlinear excitations (LNEs), thereby suggesting that these systems allow engineering of preferential energy distribution over extended times.

Introduction. – The Fermi-Pasta-Ulam-Tsingou (FPUT) chain held between fixed end walls was examined in the *weakly* nonlinear regime in 1955 [1]. In this system, masses are connected by nearest-neighbor springs where the springs are characterized by quadratic, cubic (α-FPUT), and/or quartic (β-FPUT) interactions. The original study [1] showed that there was an apparent lack of equipartitioning of energy at late times when harmonic modes were activated as initial conditions. That equipartitioning was achieved was later settled by Livi *et al.* [2,3], and others [4–12]. In 1965, Zabusky and Kruskal [13] argued that the α-FPUT system in the continuum limit could be framed as a Korteweg-de Vries problem (an integrable system) and should admit solitons. Study of solitons using various integrable systems has since received attention [14–17].

Much less is known about the dynamics of the β-FPUT chain in the *strongly* nonlinear regime where the coefficient of the harmonic term is very small compared to the coefficient of the nonlinear term in the potential [18–25]. This regime has been extensively probed in recent years for the intrinsically nonlinear Hertz potential in the context of granular systems [26–31] and for the FPUT system [25]. *An interesting possibility in this regime concerns a tendency to temporarily localize excitations.* We systematically address the energy localization behavior in the fully nonlinear and strongly nonlinear regimes in this letter.

We first briefly discuss the properties of and then characterize the solitary waves (SWs) that develop in the fully nonlinear regime. This is followed by a discussion on the SW-like objects as a function of progressively stronger harmonic interactions. We next focus on how energy localization happens due to *interactions* between the SWs, and propose new analytic descriptions of the SW itself and of the SW collision problem to describe the physics associated with the energy localization. We show that such collisions can lead to localized excitations in the collision region. The effects of inserting appropriate "decorations" in the chain are then discussed. We suggest that it may be possible to prepare one or more energy traps, which can hold a substantial amount of the total energy of the system for extended times. Finally, we address the issue of trapping for weakly harmonic interactions in addition to the strongly nonlinear interactions. We contend that decorations can be invoked to substantially alter mechanical energy distribution in strongly nonlinear β-FPUT chains for extended times [32].

Model and calculational details. – The Hamiltonian of the system is given by $H = \sum_{i=1}^{N-1}[p_i^2/2m_i + V(|x_{i+1} - x_i|)]$, where we use the notation

$$V(|x_{i+1} - x_i|) = \frac{\alpha}{2}(x_{i+1} - x_i)^2 + \frac{\beta}{4}(x_{i+1} - x_i)^4. \quad (1)$$

Before proceeding further, we note that in the original FPUT work and in most subsequent works, α and β were used as coefficients of the *cubic and quartic* terms in $V(|x_{i+1} - x_i|)$, respectively, and that the coefficient of the

quadratic term was set to unity. In those works, the coefficients of the nonlinear terms were $\ll 1$. Here, however, we will be studying the strongly nonlinear regime. Our unconventional choice of parameters in eq. (1) is therefore due to our natural need to have a coefficient associated with the quadratic term that can be varied.

We let the number of particles $N = 1000$, 500 or 100 depending upon the calculations involved in the simulations. The particle masses are set to unity henceforth except at the two ends, where $x_0 = x_{N+1} = 0$ at all times (effectively making their masses infinite). The simulations below have been carried out using a velocity-Verlet integration algorithm [33]. The bond length, which only sets a minimum of the energy scale, has not been explicitly used as a parameter but this means that α and β set the energy scale of the system. In most of our integrations, the time step was $\Delta t = 10^{-6}$. We have also used Δt as small as 10^{-10} and others in between to make sure our choice of time steps incurs negligible roundoff error. For $\Delta t = 10^{-6}$, we typically have made runs across $\sim 10^9$ to $\sim 10^{10}$ time steps. The typical energy accuracy we have managed to maintain is ~ 1 part in 10^7.

As we shall see below, we will use SW collisions in pristine and in decorated chains to realize energy localization in the strongly nonlinear FPUT system. The decorations in our studies are achieved by altering one or more springs such that they can oscillate at higher frequencies than others when excited. The decoration will be defined at a location where the potential is $V'(x_i - x_{i+1}) \equiv \kappa_i V(x_i - x_{i+1})$. Observe that similar dynamics can be obtained by varying the masses of the particles as well. One simple way to decorate would be to insert a "wall" in the potential energy located in the center of the chain by setting $\kappa_{50} = \kappa_{51} = 2$ and $\kappa_i = 1$ otherwise. Typically we will use wider traps, *e.g.*, $\kappa_i = (1.00, \ldots, 1.00, 1.25, 1.50, 1.75, 2.00, 2.00, 1.75, 1.50, 1.25, 1.00, \ldots, 1.00)$ for $1 \leq i \leq N-1$ to insert a decoration at the center of the chain with peak at particles 50, 51. Various other geometries for this trap – potential wells, slower increase/decrease in the parameter κ, etc. – may also be of interest. It is important to observe, however, that *if the trap region is long enough, then the system will try to make a SW in that region*, which could suppress the tendency to form a LNE. Likewise, *single impurities are too narrow to serve as effective decoration*s given that the SWs have a spatial extent associated with them. We find that a typical decorated region of 8 masses is the best for our studies. We further note that creating decorations of *decreased* κ causes energy to be trapped outside these regions and hence has not been explored further here.

SWs in the strongly nonlinear β-FPUT chain. – Relatively few works address the propagation of an excitation in the strongly nonlinear regime of the β-FPUT chain [18–21,34]. *We studied the time evolution of a δ-function velocity perturbation of magnitude v_I initiated at time $t = 0$ at the center mass of the chain* with the time evolution of the pulse dictated by the Newton's equations.

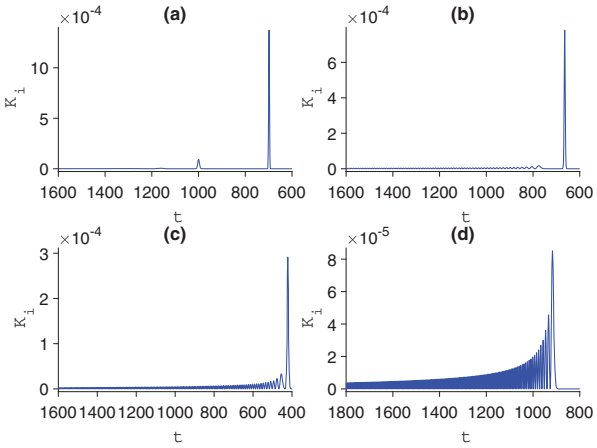

Fig. 1: (Color online) Kinetic energy of the propagating pulse taken as a function of time as the wave passes through a particle far away from impulse initiation (see text), (a) $\alpha = 0.01$, (b) $\alpha = 0.03$, (c) $\alpha = 0.05$, (d) $\alpha = 0.10$ above. The second and the following peaks form because of the rebound effect of the perturbation grain at the initiation point, almost immediately after the impact. The wide separations in (a) are due to its slower speed.

We set $N = 1000$ in these studies. Figures 1(a)–(d) show the propagating pulse by tracing out the kinetic energy *vs.* time behavior 300 particles from the initiation point in the chain for $\beta = 1$ and $\alpha = 0.01,\ 0.03,\ 0.05$ and 0.10. The SW is clearly seen for $\alpha = 0.01$ or less (not shown), whereas the development of an oscillatory tail is already evident for $\alpha = 0.03$ (figs. 1(a) and (b)). The tail becomes an essential feature of the propagating compression pulse with increasing α. Here by *compression* we mean that the leading edge of the pulse started out as a compression between the mass which was assigned the δ-function velocity v_I and its immediate neighbor in the direction in which the pulse was applied. The SW has a constant time-averaged width, as seen in the Hertz system [35]. Our results are consistent with the SW velocity $v_s \propto v_I^{1/2}$, as expected based on simple scaling arguments (see [36]). Observe that a compression pulse could also result in an opposite propagating dilation pulse. We find that for the β-FPUT chain, the dilation pulse is of identical strength to the compression pulse and moves in the opposite direction (not shown in fig. 1).

The intrinsically ($\alpha = 0$) and strongly nonlinear ($\alpha \to 0$) regimes hence exhibit SW and SW-like propagation. These waves are significantly different than in the regimes where α is significant. The velocity of the fully formed wave is measured in units of number of particles traversed/unit time. The leading edge of the pulse velocity for $\alpha > 0$ is measured for all cases and for the lengths of the runs. We find that this velocity (also called v_s) increases as α^2 for small enough α (see fig. 2) and crosses over to $\sqrt{\alpha}$ when α is sufficiently large ($\beta = 1,\ \alpha > 2$), as expected for sound propagation. We are unable to identify an analytic expression that will capture the results presented

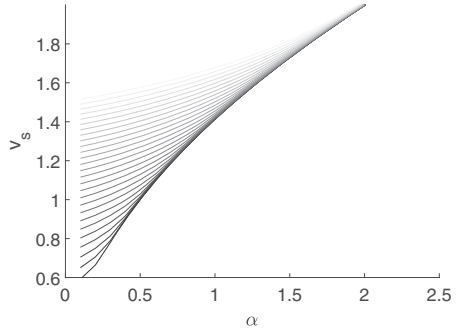

Fig. 2: (Color online) Speed of the leading edge of the pulse v_s *vs.* α for several different initial impulse values, where v_I varies between 0.3 and 3.0 from the lowest to the highest in intervals of 0.1.

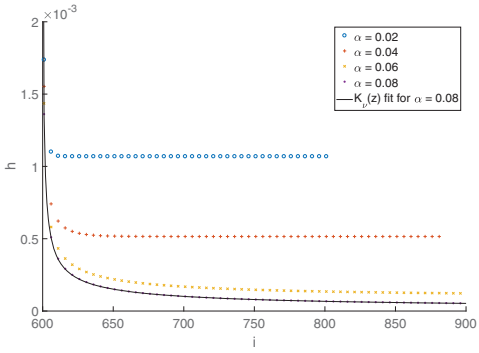

Fig. 3: (Color online) Height of the leading edge (normalized kinetic energy) *vs.* particle number for several different α values, showing the decrease in height (and therefore dispersion) of the wave shortly after the impulse as the system tends toward the acoustic limit. Top to bottom: $\alpha = 0.02, 0.04, 0.06, 0.08$.

in fig. 2.

The properties of the SW like objects in fig. 1 are complex enough that a complete characterization is yet to be made. We define the height of the leading edge of the traveling pulse at any instant as the value of its kinetic energy at the peak, normalized by the total energy of the chain: that is, $h(t) = h_i(t) = \frac{K_i(t)}{E_{tot}}$, when the wave has its peak in particle i. Since the system consists of discrete particles, the wave frequently passes between particles and the kinetic energy appears to momentarily decrease. For simplicity, we take the measurements of height when the wave's peak is on a single particle. Figure 3 shows how the height of the wave changes shortly after the perturbation. Here the velocity perturbation has taken place at particle 600. As expected, with decreasing α the wave becomes SW-like and has a constant height. With larger α, $h(i)$ begins to decay and the wave begins to disperse in space as it travels since the wave is becoming more acoustic in nature.

In this large-α regime the entire wave pulse including the tail may be closely approximated by a Bessel function (see the solution in [37]), $v_i(t) = J_\mu(\kappa t)$, where $\kappa \approx \sqrt{8\alpha}$ and the parameter μ determines the time t_i at which the leading edge of the wave reaches particle i by $t_i \approx \frac{\mu}{\kappa}$. As α increases the error in the approximation for t_i becomes smaller. We define t_i as follows: let $t_{i,1}$ be the time at which the kinetic energy of particle i reaches 0.1% of its maximum value, and let $t_{i,2}$ be the time at which it reaches its first minimum; then $t_i = \frac{t_{i,1}+t_{i,2}}{2}$. The motivation for this definition is the slight asymmetry of the leading edge.

The peaks of the tail have a full width at half-maximum $W \propto \frac{1}{\alpha^2}$. Furthermore, the height of the leading edge may be approximated by a modified Bessel function of the second kind $h(t) = K_\nu(t)$ as the wave travels [38]. This is an empirical result. Figure 3 shows the height of the leading edge for several small values of α. The modified Bessel approximation of the second kind well describes the behavior of the wave for larger values of α; and for extremely small α (less than ~ 0.05) it is clearly more reasonable to treat the height of the leading edge as a constant. The fitted modified Bessel function of the second kind is shown for the $\alpha = 0.08$ case; the function plotted is approximately $3.6 \times 10^{-5} K_{0.62}(0.003(z - 600))$. Here z is simply a continuous variable which interpolates through the discrete points i.

Now for very small values of α it is reasonable to guess that the functional form of the leading edge of our wave should be about the same as that in a fully nonlinear system. The FPUT system of course does not admit a SW solution with an exact analytic form. However, we have been able to find an approximate solution. Inspired by earlier work by one of us [28,39] we tested functions of the form $\mathrm{sech}(az)$, $\mathrm{sech}^2(az)$, etc. We found that a solution of the form $\mathrm{sech}^2(az + bz^3)$ is able to accurately describe the properties of the SW seen in the fully nonlinear ($\alpha = 0$) case of the β-FPUT chain. Figure 4 shows this function superimposed over the actual data, as well as its first several derivatives. In the next section we shall provide further verification that this function is a reasonable approximation.

Virial theorem, energy localization and SW collisions. – By invoking the virial theorem in mechanics for a system described by a potential $V \sim r^n$, where r is the inter-particle distance and $n = 4$, it can be readily shown that $\langle K \rangle = 2\langle V \rangle$, where $\langle \ldots \rangle$ denotes time average, K is the total kinetic energy, V is the total potential energy, and the average is done over a time interval that is sufficiently large (*i.e.*, ideally goes to infinity) [40]. Further, since the β-FPUT system is expected to eventually reach equipartition [41], the same relationship between $\langle K \rangle$ and $\langle V \rangle$ should be valid in equipartition as well. It would be reasonable to infer then that the fully nonlinear FPUT system has some preference for moving energy (such as via SWs) as opposed to localizing energy. On the contrary in a fully harmonic system ($\beta = 0$), $\langle K \rangle = \langle V \rangle$) and hence localized harmonic excitations are easier to form. We believe this is why forming localized excitations can be challenging in these strongly nonlinear systems.

Interestingly, if the dynamics of the β-FPUT chain are

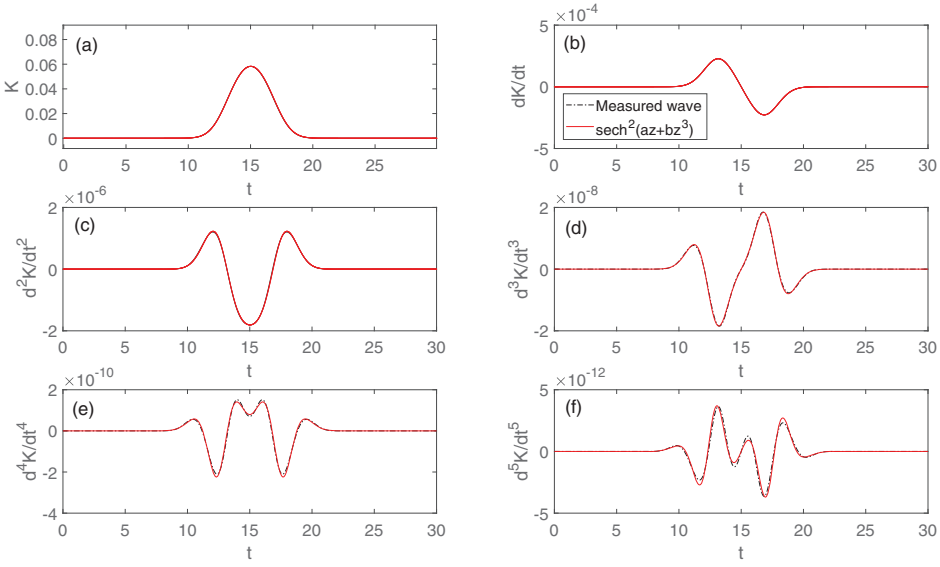

Fig. 4: (Color online) (a) The leading edge of the wave as it passes through a single particle (kinetic energy *vs.* time); $\text{sech}^2(az + bz^3)$ fit overlaid atop actual data (see text). (b)–(f) Second and higher derivatives of the function.

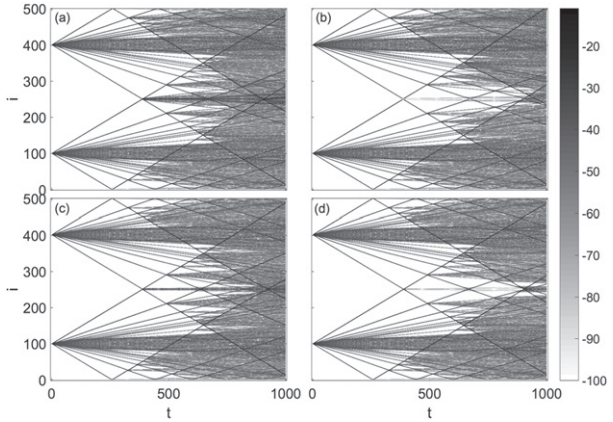

Fig. 5: (Color online) Kinetic energy *vs.* space and time, showing creation of NLEs in the center of the chain in each case. (a) Odd SW-ASW collision; $v_{100} = v_{400} = 0.4$. (b) Odd SW-SW collision; $v_{100} = -v_{400} = 0.4$. (c) Even SW-SW collision; $v_{100} = -v_{401} = 0.4$. (d) Even SW-ASW collision; $v_{100} = v_{401} = 0.4$. Gray scale: $10 \log_{10}(KE)$.

initiated with the stretch or squeeze of a bond or bonds within the chain, the system is unable to quickly disperse all the stored energy to restore $\langle K \rangle = 2\langle V \rangle$. More remains to be done to understand the details of the long-time decay of LNEs for $\alpha = 0$ and for $\alpha > 0$. Energy leakage from a LNE is discussed in ref. [25].

The nature of the energy leakage from a LNE is dependent on α. We first describe below the $\alpha = 0$ case. For simplicity we study collisions of SWs that carry the same energy and hence move at equal speeds and meet at the center of the system, whether that turns out to be on a mass or a bond. This is what we show via kinetic energy *vs.* time and space plots in fig. 5 as described in the caption. In (a) a SW from below and an ASW from above meet at a mass, thus pushing the mass in the same direction with twice its usual amplitude and localizing energy in the two bonds connected to the central mass and the mass itself to generate a LNE. In (b) two SWs meet in a central mass, squeezing two adjacent bonds connected to this mass and localizing some kinetic energy, thereby initiating oscillations to make a LNE. In (c) two SWs meet in a central bond and squeeze the same to initiate a LNE. In (d), a SW and an ASW meet at a central bond, thereby displacing the bond in one direction and generating a weak LNE.

These collisions can be used to verify the accuracy of the $\text{sech}^2(az + bz^3)$ solution for the displacement of the SW from the previous section. For $v_i = 0.4$, we use $0.2328\ \text{sech}^2(0.7884z + 0.1056z^3)$. We find that as α increases, b/a becomes smaller until we reach a point where α is large enough such that the above function is no longer appropriate. Each of the collisions have been repeated using $\text{sech}^2(az + bz^3)$ waves rather than the natural FPUT SWs, in order to verify that the energy content remaining in the central bond after the collision is the same and that the LNE formation is unaffected. Figure 6 shows the result of the first collision (a). We have obtained similar results in the other three cases and, therefore, they are not shown.

Now let us return to the original subject of SW collisions in the FPUT system. Since we are interested in generating strong localized excitations in this system, we focus on the details of the SW-SW collision where the SWs meet at a bond and initiate a LNE (once again (a) from above). It is reasonable to expect that sufficiently large amplitude of the colliding SWs would raise the frequency of oscillations in the bond of interest and generate a long lived LNE and this is what we see. As discussed in [25], higher frequencies take longer to disperse. Hence we would ex-

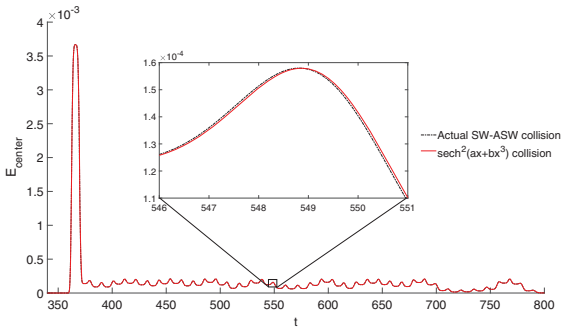

Fig. 6: (Color online) The total energy located in the central bond and its connected particles after an odd SW-ASW collision (as per (a) of fig. 5). The energy has been calculated by summing the kinetic energy of the central particle with the potential energies of its connected bonds, $E_c = 1/2mv_c^2 + V(|x_c - x_{c-1}|) + V(|x_c - x_{c+1}|)$. The solid line represents the result of the same collision as performed with $\mathrm{sech}^2(az + bz^3)$ functions rather than δ-function velocity perturbations (dashed line). The error is of the order of 1 part in 100.

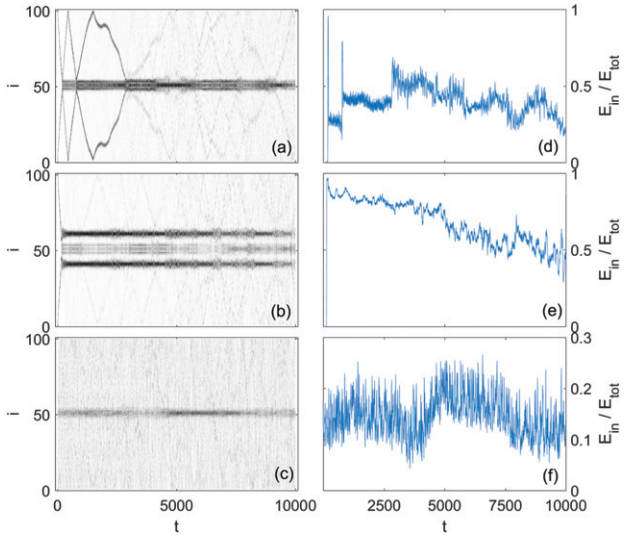

Fig. 7: (Color online) (a), (b), (c): kinetic energy *vs.* space and time for the three types of traps described in the text. Darker colors correspond to higher energies with black being a kinetic energy magnitude of 0.01. (d), (e), (f): E_{in}/E_{out} denote the fraction of the total energy *vs.* time within the decorated regions of (a), (b), and (c), respectively (see text).

pect the LNEs thus made to be more stable. We do not study the collisions involving SWs and ASWs when they carry unequal amounts of energy here. It turns out that energy localization via collisions of SWs and ASWs is seen in such cases as well with the main difference that the high frequency oscillations that result in such collisions tend to carry some momentum and hence show some drift.

Stiffer bonds would need sufficiently large amplitudes of stretch to get excited and once appropriately perturbed, they tend to disperse their energy slowly [25]. Consistent with this observation, our studies show that the SWs have a tendency to get reflected by stiffer bonds. To efficiently trap energy in regions where SWs meet, we hence stiffen the bonds gradually in the region where the SWs meet. The κ values discussed in the model and calculational details section are for the bonds in this region.

Wave collisions for $\alpha \neq 0$ in the β-FPUT chain. – Studies of the β-FPUT system using particle dynamics simulations have earlier shown that $\alpha > 0$ tends to stabilize the LNEs in the sense that they decay more slowly [24]. For this reason our simulations use a value of $\alpha = 0.1$ in the studies described in fig. 7. For $\alpha = 0.1$, the perturbations initiated at time $t = 0$ resemble a SW with an oscillatory tail as shown in fig. 1. We would loosely describe these as SWs and for the most part ignore the oscillatory tails, which lead to some bending of the SWs in space and time (see fig. 7(a) between $t = 0$ and $t \approx 200$ for example). As alluded to above the decorated bonds which are placed between masses 47 and 54 allow for leaving some energy in the decoration and backscatters the rest as seen around $t \approx 200$. Such backscattering is seen many times after that in fig. 7(a). In fig. 7(d) we may see that the first SW leaves approximately a fifth of its energy in the trap; the second wave arriving shortly thereafter leaves a similar portion. Notice the visible slowdown in the speed of the backscattered SW at $t \approx 1000$. Once the energy is in the trap its decay is very slow. The initial stages of the decay of a LNE are addressed in ref. [25]. However, later stages are not well understood. It is, however, seen that the LNE tries to emit stable SW-like structures and has a mixed degree of success in doing so, emitting intermittent unstable propagating structures and stable SW-like structures at others. The rest of its energy stays within the decorated region and continues to reflect back and forth across the interior boundaries of the decoration, causing localization. The decay of the LNEs are hence affected by the boundaries. The time evolution of the LNE is sufficiently noisy that the form of its energy decay is not clear from our studies here. The LNEs live for the entire length of our simulations in every case we studied.

It is instructive to examine the interaction of a SW with the decoration rather than that of two equal and opposite SWs. Figure 7(b) shows an example of this. Here we take a system which has precisely the same parameters and initial conditions as that of the system in fig. 7(a). However, we place *three* identical decorations instead of one, each region being separated by two particles. These decorations are placed at particles 37-44, 47-54, and 57-64. In fig. 7(b) we can see a SW encounter the decorated region and then get largely entrapped by the other end of the trap.

The central decoration in fig. 7(b) traps the energy that managed to penetrate the first decorated region but, as expected, the magnitude of energy localization is less than that in the decorated regions outside the central region. Thus, multiple decorations can indeed be invoked for localizing significant amounts of energy for finite times

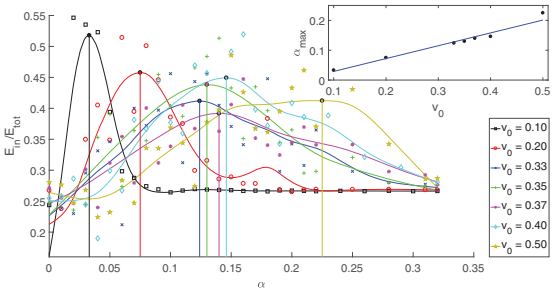

Fig. 8: (Color online) Time-averaged energy present within the trapping region for various values of α and v_0. Inset: α value corresponding to the maximum energy trapping *vs.* v_0.

in the β-FPUT system. For more clarity we plot the total amount of localized energy (E_{in}/E_{out}) in the decorated regions in this system as a function of time t in fig. 7(e). Nearly all this energy ends up being trapped initially. As expected, this energy slowly leaks out to the rest of this system as it did in the system in fig. 7(a), the linear fit to this decay over short times has the slope $-4.9 \pm 0.4 \times 10^{-5}$ in units of inverse time, which is larger than that in the single-decorated-region study above. Thus, increasing the number of decorations appears to raise short-term localization but energy attenuation from these regions also increases. Regardless, it is encouraging to see that the decorations can effectively localize energy in β-FPUT systems.

Is it possible to extend the energy localization problems when arbitrary perturbations are initiated into the system with one or more decorated regions? To answer this we set up one decorated region between masses 47 and 54 in a chain where each mass is given a velocity perturbation with magnitude uniformly randomly distributed between $v_0 = -0.1$ and 0.1. The plot of kinetic energy *vs.* space and time in fig. 7(c) shows that even for highly random perturbations one sees energy localization in the middle of the system, albeit localization which carries low energy and fluctuates significantly throughout the run as evident from fig. 7(f).

A detailed analysis of the localization seen in fig. 7(a) is shown in fig. 8. Here we measure the energy within the decorated region described by E_{in}/E_{tot} for various values of α and v_0 with $\beta = 1$. The inset in fig. 8 reveals that $\alpha_{max} = Av_0 + B$, where α_{max} is the value of α which maximizes localization for a given v_0 and $A = 0.43 \pm 0.06$ and $B = -0.014 \pm 0.004$ in system units. Smoothing has been performed on this data to better understand the dependence of E_{in}/E_{out} on α. The three main effects to note from fig. 8 are that 1) weak SWs tend to trap energy only within a small range of α, that 2) strong SWs trap a smaller proportion of their energy but are *less sensitive* to α, and that 3) the α value where maximum trapping occurs increases with the SW energy.

The three observations above can be related together as follows. First, we see from fig. 8 that in the $v_0 = 0.10$ case trapping is significant and occurs only for a narrow range of small values of α. In this case there is almost no wave train and the object which encounters the trap is a single pulse with small amplitude. If we suppose that a given trap *only* traps waves at a certain critical amplitude, then it is quite easy to explain the rest of fig. 8: that the larger values of v_0 and α create waves which mostly pass through the trap, and that a portion of their wave train which matches most closely to what the trap prefers remains in that region.

As α increases for a wave with small v_0, we would then expect to see that energy trapping would vanish as energy moves from the leading edge of the wave packet to the wave train causing every peak in the object to decrease below the critical amplitude – and this is exactly what we observe in fig. 8.

For a wave which has large v_0 we would expect to see almost no trapping for *small* values of α as the SW would have amplitude larger than the critical value. Furthermore, we would expect that, as α increases causing the leading edge of the wave to donate its energy to its wave train, energy trapping would occur at *every part* of the wave train that is close to the critical amplitude. And again this is exactly what is seen in fig. 8 as the range in α over which energy trapping occurs is wider for larger v_0. Thus, using adjacent multiple traps, as in fig. 7(b), is likely to be an effective strategy to localize impulses in β-FPUT chains. Use of sets of such traps could provide a way to accomplish preferential energy distribution and localization over extended times in strongly nonlinear, non-integrable systems such as the one considered here. We envision that similar trapping mechanisms can also be invoked to realize energy localization in interacting strongly nonlinear, non-integrable systems such as quantum spin chains which have been of much recent interest [42].

Summary and conclusions. – In this letter we have examined how collisions between SWs in the strongly nonlinear β-FPUT system naturally create LNEs. We have proposed an analytic solution to describe the SWs and have demonstrated that the solution correctly describes collisions between SWs. The role of a weak harmonic term in the β-FPUT chain has been studied and we show that LNEs can be sustained for extended times for small values of α. Long-term energy localization in a chain with the right distribution of extended traps for various values of α is also possible as discussed above and is a natural consequence of the interactions between the SWs among each other and the traps in the β-FPUT system. It is hence conceivable that strongly nonlinear, non-integrable systems such as the β-FPUT system can be potentially explored for applications in mechanical energy harvesting.

* * *

We thank Michelle Przedborski and Rahul Kashyap for their interest in this work.

REFERENCES

[1] Fermi E., Pasta J. and Ulam J., *Studies of nonlinear problems*, LA-1940, Los Alamos National Lab, May 1955.
[2] Livi R. *et al.*, *Phys. Rev. A*, **31** (1985) 1039.
[3] Livi R. *et al.*, *Phys. Rev. A*, **31** (1985) 2740.
[4] Kantz H. *et al.*, *J. Stat. Phys.*, **76** (1994) 627.
[5] De Luca J., Lichtenberg A. J. and Lieberman M. A., *Chaos*, **5** (1995) 283.
[6] De Luca J., Lichtenberg A. J. and Ruffo S., *Phys. Rev. E*, **51** (1995) 2877.
[7] Ullmann K., Lichtenberg A. J. and Corso G., *Phys. Rev. E*, **61** (2000) 2471.
[8] Casetti L. *et al.*, *Phys. Rev. E*, **55** (1997) 6566.
[9] Gershgorin B., Lvov Y. V. and Cai D., *Phys. Rev. E*, **75** (2007) 046603.
[10] Onorato M. *et al.*, *Proc. Natl. Acad. Sci. U.S.A.*, **112** (2015) 4208.
[11] Reigada R., Sarmiento A. and Lindenberg K., *Phys. Rev. E*, **64** (2001) 066608.
[12] Reigada R., Sarmiento A. and Lindenberg K., *Phys. Rev. E*, **66** (2002) 046607.
[13] Zabusky N. J. and Kruskal M. D., *Phys. Rev. Lett.*, **15** (1965) 240.
[14] Kivshar Y. S. and Malomed B. A., *Revs. Mod. Phys.*, **61** (1989) 763.
[15] Manakov S. V., *Sov. Phys. JETP*, **40** (1975) 269.
[16] Wadati M., *Pramana - J. Phys.*, **57** (2001) 841.
[17] Campbell D. K., Rosenau P. and Zaslavsky G. M., *Chaos*, **15** (2005) 01501.
[18] Friesecke G. and Pego R., *Nonlinearity*, **12** (1999) 1601.
[19] Friesecke G. and Pego R., *Nonlinearity*, **15** (2002) 1343.
[20] Friesecke G. and Pego R., *Nonlinearity*, **17** (2004) 207.
[21] Friesecke G. and Pego R., *Nonlinearity*, **17** (2004) 229.
[22] Pankov A., *Traveling Waves and Periodic Oscillations in Fermi-Pasta-Ulam Lattices* (Imperial College, London) 2005.
[23] Sen S. and Krishna Mohan T. R., *Phys. Rev. E*, **79** (2009) 036603.
[24] Krishna Mohan T. R. and Sen S., *Pramana - J. Phys.*, **77** (2011) 975.
[25] Kashyap R. *et al.*, *Int. J. Mod. Phys. B*, **31** (2017) 1742014.
[26] Nesterenko V., *J. Appl. Mech. Tech. Phys.*, **5** (1983) 733.
[27] Sinkovits R. S. and Sen S., *Phys. Rev. Lett.*, **74** (1995) 2686.
[28] Sen S. and Manciu M., *Phys. Rev. E*, **64** (2001) 056605.
[29] Rosas A. and Lindenberg K., *Phys. Rev. E*, **69** (2004) 037601.
[30] Coste C., Falcon E. and Fauve S., *Phys. Rev. E*, **56** (1997) 6104.
[31] Ahnert K. and Pikovsky A., *Phys. Rev. E*, **79** (2009) 026209.
[32] Przedborski M., Harroun T. and Sen S., *Appl. Phys. Lett.*, **107** (2015) 244105.
[33] Allen M. P. and Tildesley D. J., *Computer Simulation of Liquids* (Clarendon, Oxford) 1987.
[34] Flytzanis N., Pnevmatikos S. and Peyrard M., *J. Phys. A*, **22** (1989) 783.
[35] Sun D. and Sen S., *Granular Matter*, **15** (2013) 157.
[36] Sen S. *et al.*, *Phys. Rep.*, **462** (2008) 21.
[37] Rosas A. and Lindenberg K., *Phys. Rev. E.*, **68** (2003) 041304.
[38] Abramowitz M. and Stegun I., *Handbook of Mathematical Functions* (Dover, New York) 1987.
[39] Sen S. and Manciu M., *Physica A*, **268** (1999) 644.
[40] Goldstein H., Poole C. and Safko J., *Classical Mechanics* (Addison-Wesley, San Francisco) 2002, p. 86.
[41] Benettin G. and Ponno A., *J. Stat. Phys.*, **144** (2011) 793.
[42] Neyenhuis B. *et al.*, *Sci. Adv.*, **3** (2017) e1700672.